N^6-methyladenosine Binding Proteins Negatively Regulate HIV-1 Infectivity and Viral Production

Wuxun Lu [1, #], Nagaraja Tirumuru [1, #], Pratibha C. Koneru [2], Chang Liu [3, 4], Mamuka Kvaratskhelia [2], Chuan He [3, 4], and Li Wu [1, *]

[1] Center for Retrovirus Research, Department of Veterinary Biosciences, The Ohio State University, Columbus, Ohio, United States of America (USA)

[2] Division of Infectious Diseases, University of Colorado School of Medicine, Aurora, Colorado, USA

[3] Department of Chemistry, Department of Biochemistry and Molecular Biology, Institute for Biophysical Dynamics, The University of Chicago, Chicago, Illinois, USA

[4] Howard Hughes Medical Institute, The University of Chicago, Chicago, Illinois, USA

[*]Correspondence author

E-mail: wu.840@osu.edu (LW)

[#] These authors contributed equally to this work.

Short title: m^6A-binding proteins inhibit HIV-1 infectivity

Abstract (288 words)

The internal N^6-methyladenosine (m^6A) modification of cellular mRNA regulates post-transcriptional gene expression. The YTH domain family proteins (YTHDF1-3, or Y1-3 for short) bind to m^6A-modified cellular mRNA and modulate its metabolism and processing, thereby affecting protein translation in cells. We previously reported that HIV-1 RNA contains m^6A modification and that Y1-3 proteins inhibit HIV-1 infection by decreasing HIV-1 reverse transcription. Here we extended our studies to better understand the mechanisms of Y1-3-mediated inhibition of HIV-1 infection and viral production. Overexpression of Y1-3 proteins in target cells decreased HIV-1 genome RNA (gRNA) levels and inhibited early and late reverse transcription. Purified recombinant Y1-3 proteins preferentially bound to the m^6A-modified 5' leader sequence of gRNA compared with its unmodified RNA counterpart, consistent with the strong binding of Y1-3 to HIV-1 gRNA in infected cells. HIV-1 mutants with two altered m^6A modification sites in the 5' leader sequence of gRNA demonstrated significantly lower infectivity compared with wild-type HIV-1, suggesting that these sites are important for viral infection. Interestingly, HIV-1 produced from cells with knockdown of endogenous Y1 and Y3 proteins had increased viral infectivity, while HIV-1 produced from cells with overexpression of Y1-3 proteins showed reduced viral infectivity. We demonstrated that Y1-3 proteins and HIV-1 Gag formed a complex with RNA in cells. Furthermore, HIV-1 produced from cells treated with an inhibitor to block m^6A modification showed a 3-fod decrease in m^6A level of HIV-1 RNA, but a 3-fold increase in viral infectivity compared to HIV-1 produced from mock-treated cells. These results suggest the inhibitory effects of Y1-3 proteins on HIV-1 infection and provide new insight into the mechanisms of m^6A modification of HIV-1 RNA in regulating viral replication, which clarify some discrepancies in the previously published studies in this area.

Author Summary (186 words)

Cellular RNAs have over 100 distinct modifications regulating gene expression, in which m^6A modification is the most abundant. Although m^6A modification has been identified in various viruses, its role in HIV-1 replication and protein expression was recently recognized. The effects of m^6A-binding proteins (termed Y1-3) on HIV-1 infection and the underlying mechanisms remain unclear. Here we show that Y1-3 proteins inhibit HIV-1 infection through reduction of HIV-1 genomic RNA and reverse transcription. Y1-3 proteins preferentially bind to an m^6A-modified HIV-1 RNA fragment compared with its unmodified counterpart. We found that the m^6A sites in the 5' leader sequence of HIV-1 RNA are important for viral infectivity. Overexpression of Y1-3 proteins leads to decreased infectivity of produced HIV-1, while knockdown of Y1 and Y3 proteins increase viral infectivity. Y1-3 proteins and HIV-1 Gag protein interact with RNAs and form a complex in cells. Furthermore, HIV-1 produced from cells treated with an inhibitor to block m^6A addition showed a reduced m^6A level in HIV-1 RNA, but significantly increased viral infectivity. Our findings help better understand how Y1-3 proteins inhibit HIV-1 replication through specific binding to m^6A-modified viral RNA.

Introduction

Among the more than 100 distinct modifications identified in mRNAs in different organisms, N^6-methyladenosine (m^6A) methylation is the most prevalent internal modification, accounting for 0.1% of adenosines in mammalian mRNAs (1). The dynamic addition, removal, and recognition of m^6A in cellular RNAs are coordinately regulated by three groups of host proteins, including methyltransferases (termed writers), demethylases (erasers), and m^6A-binding proteins (readers). The writers include methyltransferase-like 3 (METTL3), methyltransferase-

like 14 (METTL14), and Wilms tumor 1-associated protein (WTAP), while erasers include fat mass and obesity-associated protein (FTO) and alkB homologue 5 (ALKBH5) (2). The readers are YT521-B homology (YTH) domain family proteins (YTHDF1, YTHDF2, YTHDF3 and YTHDC1) that specifically recognize m^6A modification via a conserved m^6A-binding pocket in the YTH domain (3-5). These reader proteins modulate m^6A-modifed mRNA stability and translation, therefore playing an important role in modulating post-transcriptional gene expression (6-10).

Three recent studies highlighted the importance of m^6A modifications of HIV-1 RNA in regulating viral replication and gene expression (11-13). Despite some consistent results, there are discrepancies in the locations, effects, and mechanisms of m^6A modification of HIV-1 RNA in these studies (11-13). Our published study identified m^6A modifications in the 5' and 3' un-translated regions (UTRs), as well as in the *rev* and *gag* genes of the HIV-1 genome (13). We previously reported that overexpression of Y1-3 proteins in cells inhibits HIV-1 infection by primarily decreasing HIV-1 reverse transcription, while knockdown of endogenous Y1-3 in Jurkat $CD4^+$ T-cell line or primary $CD4^+$ T-cells increases HIV-1 infection (13). However, the underlying mechanisms of Y1-3-mediated inhibition of HIV-1 infection remain unclear.

Here we report that Y1-3 inhibited HIV-1 infection in target cells by lowering viral genome RNA (gRNA) levels and reverse transcription products. We demonstrate that the m^6A-modified HIV-1 RNA fragment preferentially bound to Y1-3 proteins compared with an un-modified RNA counterpart, and mutations of two m^6A sites in the 5' UTR significantly decreased viral infectivity. Knockdown and overexpression of Y1-3 proteins in virus-producing cells positively and negatively modulated HIV-1 infectivity, respectively. Y1-3 proteins and HIV-1 Gag protein formed a complex with RNAs in cells. Furthermore, HIV-1 produced from

93 cells treated with an inhibitor to block m^6A addition showed a reduced m^6A level in HIV-1
94 RNA, but increased viral infectivity. Together, these data suggest new mechanisms by which
95 Y1-3 mediate HIV-1 inhibition during early steps of the viral life cycle.
96
97 **Results**
98 **Overexpression of Y1-3 proteins inhibits HIV-1 infection by decreasing HIV-1 gRNA level**
99 **and inhibiting viral reverse transcription**
100 Our previous study showed that Y1-3 proteins negatively regulate HIV-1 post-entry
101 infection in target cells, including primary $CD4^+$ T-cells (13). To better understand the
102 underlying mechanisms, we compared HIV-1 gRNA levels, early and late reverse transcription
103 (RT) products in cells overexpressing individual Y1-3 proteins and control cells after HIV-1
104 infection. We first used vesicular stomatitis virus glycoprotein (VSV-G)-pseudotyped single-
105 cycle HIV-1 expressing firefly luciferase to infect HeLa cells stably expressing each individual
106 Y1-3 proteins (HeLa/Y1-3) or control cells transduced with an empty vector (HeLa/Vector).
107 Consistent with our previous results (13), Y1-3 overexpression (Fig. 1A) resulted in significantly
108 lower levels of HIV-1 postentry infection (26%, 8.6%, and 23% in HeLa/Y1, HeLa/Y2 and
109 HeLa/Y3 cells, respectively) compared with HeLa/Vector control cells (set as 100%, Fig. 1B).
110 To examine whether Y1-3 proteins alter the levels of HIV-1 gRNA in the infected cells,
111 HeLa/Y1-3 or control cells were infected with single-cycle HIV-1 and total RNAs from the cells
112 were isolated at 1, 3, and 6 h post-infection (hpi). The levels of HIV-1 gRNA were quantified
113 using RT-qPCR (14). At each time point tested, HIV-1 gRNA levels were lower in HeLa/Y1-3
114 relative to those in HeLa/Vector control cells, and HIV-1 gRNA level gradually declined after

infection as expected (Fig. 1C). These results indicate that overexpression of Y1-3 proteins leads reduced levels of HIV-1 gRNA, likely by decreasing viral RNA stability.

Our previous study showed that Y1-3 proteins inhibit accumulation of HIV-1 late RT products in infected cells (13), while it is unclear whether Y1-3 proteins affect HIV-1 early RT efficiency. To address this question, HeLa/Y1-3 cells or HeLa/Vector control cells infected by HIV-1-Luc/VSV-G were collected at 6, 12 and 24 hpi for quantification of HIV-1 early and late RT products by quantitative PCR (qPCR) (15). At each time point, the levels of both early and late RT products were significantly lower in HeLa/Y1-3 cells compared with vector control cells (Fig. 1D and 1E). Compared with vector control cells at 6 hpi, Y1-3 overexpression decreased HIV-1 gRNA levels, and further decreased early and late RT products (Fig. 1C-E), suggesting that overexpression of Y1-3 proteins decreases viral gRNA stability and inhibits early RT product synthesis. At 24 hpi, the levels of early and late RT products decreased to 37-54%, while HIV-1 infection decreased to 8.6-26% in HeLa/Y1-3 cells compared with vector control cells (set to 100%, Fig. 1B, 1D and 1E). These data suggest that, in addition to reverse transcription, overexpression of Y1-3 proteins in cells can also negatively regulate HIV-1 gene expression.

Overexpression of Y1-3 proteins in HeLa/CD4 cells inhibits wild-type (WT) HIV-1 replication

Since the *firefly luciferase* gene in HIV-1-Luc/VSV-G virus has consensus sequences recognized by m^6A writers, its mRNA may also have m^6A modifications. To exclude the effects of m^6A modification of *luciferase* mRNA on HIV-1 infection, we used WT, replication-competent HIV-1_{NL4-3} to infect HeLa cells overexpressing CD4 and individual Y1-3 proteins (HeLa/CD4/Y1-3) or vector control cells. Using flow cytometry, we confirmed that the majority

of these cells were double positive for the HIV-1 primary receptor CD4 and co-receptor CXCR4 (71-81%), which would allow efficient fusion-mediated viral entry (Fig. 2A). Immunoblotting results also confirm that HeLa/CD4/Y1-3 cells stably expressed FLAG-tagged individual Y1-3 proteins (Fig. 2B). In order to examine the effects of Y1-3 overexpression on HIV-1 replication in the full viral lifecycle, we collected infected cells at 72 hpi for further analyses (Fig. 2C-F). Consistent with the results from single-cycle HIV-1-Luc/VSV-G (Fig. 1B), Y1-3 overexpression efficiently inhibited infection of WT HIV-1_{NL4-3} as Gag protein levels in cells and p24 (capsid) levels in supernatants were significantly lower in HeLa/CD4/Y1-3 cells compared with vector control cells (Fig. 2B and 2C). These results confirmed inhibitory effects of Y1-3 proteins on HIV-1 infection, and suggested that the inserted *luciferase* gene in HIV-1-Luc/VSV-G does not affect the observed phenotype. Infection of HeLa cells overexpressing Y1-3 proteins with WT HIV-1 also resulted in significantly lower early and late HIV-1 RT products (Fig. 2D and 2E, respectively), and consequently reduced *gag* mRNA levels compared with vector control cells (Fig. 2F). These data suggest that Y1-3 proteins inhibit WT HIV-1_{NL4-3} infection before or during the RT stage.

YTHDF1-3 proteins specifically bind to HIV-1 gRNA in infected cells

To confirm Y1-3 binding to HIV-1 gRNA in infected cells, we performed immunoprecipitation (IP) of Y1-3 in HeLa/CD4/Y1-3 cell lines and vector control cells infected with WT HIV-1_{NL4-3} (Fig. 3A). To validate the specificity of Y1-3 binding to HIV-1 RNA, we also included a Y1-3 unrelated cellular protein MAL (MyD88 adapter-like, also known as Toll/IL-1 receptor (TIR) domain-containing adapter protein, or TIRAP) (16, 17) as an additional negative control in the IP assay (Fig. 3A). We then quantified the amounts of Y1-3-bound HIV-1

gRNA using RT-qPCR assays (13). We observed that Y1-3 specifically and efficiently bound to WT HIV-1 gRNA in HIV-1_{NL4-3} infected HeLa/CD4/Y1-3 cells compared with vector control or MAL-expressing cells (Fig. 3B). The levels of HIV-1 gRNA bound to Y1 appeared higher than those bound to Y2 and Y3 (Fig. 3B), which could be due to the higher expression of Y1 in HeLa/CD4 cells relative to Y2 and Y3 proteins (Fig. 3A) and consequently a higher level of IP products (Fig. 3B). These data indicate that Y1-3 proteins specifically bind to WT HIV-1_{NL4-3} gRNA in infected cells.

Y1-3 proteins preferentially bind to an m^{6}A-modifed HIV-1 RNA fragment *in vitro*

Our previous study showed that HIV-1 RNA contains m^{6}A modifications at both the 5' and 3' UTR (13). Given the critical role of the 5' UTR in initiation of HIV-1 reverse transcription, in this study we focused on the m^{6}A sites in the 5' UTR of HIV-1 gRNA. The GGACU motif is the most predominant sequence for m^{6}A modification (18, 19). The m^{6}A peak detected by high-throughput RNA sequencing in the 5' UTR of HIV-1 gRNA harbors two GGACU motifs (13). The first one is located in the primer-binding site (PBS), and the second is in upstream region of the dimer initiation sequence (DIS) (Fig. 4A). These two GGACU motifs overlap with m^{6}A modifications in HIV-1 gRNA and are close to Y1-3 protein-binding peaks identified in the 5' UTR of HIV-1 gRNA (13).

To study the binding properties of Y1-3 proteins to HIV-1 RNA with m^{6}A modification, we synthesized two RNA fragments corresponding to nucleotides 235-281 of HIV-1_{NL4-3} gRNA with or without m^{6}A modification in the second GGACU motif located in the 5' UTR (Fig. 4A). To eliminate RNA dimerization in our binding assays, the underlined DIS sequence (AAGCGCGC) was replaced with the nucleotides GAG (Fig. 4A and 4B). We first used the

AlphaScreen assay (20) to detect interaction of synthesized RNA fragments with purified full-length recombinant Y1-3 proteins. Each of these Y1-3 proteins exhibited clear preference for binding to m^{6}A-modified HIV-1 RNA than its unmodified counterpart (Fig. 4C). We further investigated *in vitro* binding of the RNA fragments to Y1-3 protein using affinity pull-down experiments. Streptavidin-conjugated beads were used to pull-down biotin-modified control or m^{6}A RNA fragments. Consistently, at lower Y1-3 concentrations (1-25 nM), clear preferences were seen for binding to m^{6}A-modified HIV-1 RNA relative to control RNA, though both RNA fragments had detectable binding to Y1-3 proteins at higher concentrations (125-625 nM) (Fig. 4D). The immunoblotting results of the pull-down experiments were quantified and normalized to 1 based on protein pull-down levels by m^{6}A RNA fragment at 625 nM protein input (Fig. 4E). To compare affinity of RNA fragments to Y1-3 proteins, we calculated the concentrations of each Y1-3 protein (ranging from 1-625 nM) required for 50% pull-down levels based on the regression curves (Fig. 4E and 4F). The 50% pull-down efficiencies indicated that Y1-3 proteins bound to m^{6}A RNA fragment 7-fold, 13-fold, and >20-fold higher than control RNA, respectively (Fig. 4F). These results demonstrate that Y1-3 proteins exhibit substantially higher affinity for m^{6}A-modified HIV-1 RNA *in vitro*, which may contribute to Y1-3-mediated inhibition of HIV-1 infection in cells.

A to G mutations in GGACU motifs of the 5' UTR of HIV-1 gRNA reduce viral infectivity

The two GGACU motifs are located in the PBS and a upstream region of the DIS (Fig. 4A), within the m^{6}A peaks of the 5' UTR of HIV-1 RNA that were identified in our previous study (13). Because the 5' UTR is critical for HIV-1 reverse transcription, genome package, and viral infectivity (21, 22), we further investigated the importance of these m^{6}A sites on HIV-1

207 replication and infection by mutagenesis. To eliminate m^6A modification of the GGACU motifs
208 in HIV-1 gRNA, A to G mutations were introduced in the first (Mut1), second (Mut2), or both
209 GGACT motifs (Mut3) in the HIV-1 proviral DNA plasmid pNL4-3 (Fig. 5A). WT pNL4-3 and
210 derived mutants (Mut1-3) were separately transfected into HEK293T cells to measure HIV-1
211 protein expression and viral release. Compared with WT HIV-1, these mutants expressed
212 comparable levels of precursor Gag protein, but the levels of cleaved p24 and intermediate Gag
213 products in cell lysates were 1.4- to 1.8-fold higher (Fig. 5B). Consistently, supernatant p24
214 levels of mutant viruses were 1.2- to 1.4-fold higher than that of WT HIV-1 (Fig. 5C), suggesting
215 a potential effect of these mutations on Gag proteolytic processing or viral release. To compare
216 the infectivity of the mutants with WT HIV-1, viruses generated in HEK293T cells with equal
217 amounts of p24 were used to infect TZM-bl indicator cells (23). Interestingly, the infectivity of
218 the mutant viruses was significantly lower (53-74%) relative to WT HIV-1 (Fig. 5D), suggesting
219 an important role of these two GGACU motifs in HIV-1 infectivity.
220 Previously published m^6A mapping results indicate that there are multiple m^6A sites in
221 different regions of HIV-1 gRNA in addition to the 5' UTR (11-13), which can potentially
222 contribute to regulating viral infectivity through interactions with Y1-3 proteins. To address this,
223 we examine whether silencing Y1-3 in target cells could restore the infectivity of these 5' UTR
224 mutant viruses. Endogenous Y1-3 proteins in TZM-bl cells were knocked down by combined
225 Y1-3 specific siRNA, and then TZM-bl cells were infected with the same p24 amount of WT or
226 mutant viruses generated from normal HEK293T cells. In TZM-bl cells with partial Y1-3
227 proteins knockdown (Fig. 5E), all three mutant viruses showed 40-50% lower infectivity relative
228 to WT HIV-1 (Fig. 5F). These results confirm the importance of these two GGACU motifs for

HIV-1 infectivity, and suggest that other m^6A sites in HIV-1 RNA can also regulate viral infectivity.

Given the important role of the PBS and DIS in structure and function of HIV-1 gRNA (24), we predicted the secondary structures of the RNA segments containing the PBS and DIS of WT and mutant viruses. Compared with the structure of WT HIV-1, the A to G mutation in the first GGACU motif (Mut1) resulted in a longer stem structure in the PBS sequence region, while mutation in the second GGACU motif did not change RNA structure containing the DIS (Fig. 5G). These data suggest that the decreased viral infectivity of Mut1 might be due to the combined effects of RNA structure change and elimination of m^6A at this site. In contrast, the reduced viral infectivity of Mut2 was likely due to elimination of m^6A modification.

Effects of Y1-3 knockdown or overexpression in virus-producing cells on HIV-1 Gag expression and viral infectivity

Our published results (13) and new data showed that Y1-3 proteins in target cells negatively regulate single-cycle and replication-competent HIV-1 infection (Fig. 1B and 2C, respectively). To further elucidate the role of Y1-3 in HIV-1 protein expression and infectivity, endogenous Y1-3 gene expression in HEK293T cells was knocked down using specific siRNAs. Compared with non-specific control siRNA, single knockdown of each Y1-3 significantly decreased HIV-1 Gag (Pr55) protein expression, and correspondingly reduced the levels of processed p24 protein in cells (Fig. 6A). Consistently, p24 levels in the supernatants of cells with single or combined Y1-3 knockdown also reduced approximately 2-fold compared with those of control cells and there was no synergistic effect of combined knockdown (data not shown).

To compare the infectivity of HIV-1 generated from cells with Y1-3 knockdown, viruses with equal amounts of p24 were used to infect TZM-bl indicator cells. As shown in Fig. 6B, viruses generated from individual Y1 or Y3 knockdown cells had significantly higher infectivity compared with virus from control cells ($P < 0.005$), suggesting that Y1 and Y3 proteins in cells negatively affect infectivity of progeny HIV-1 virions. In contrast, efficient Y2 knockdown in virus-producing cells resulted in a 25% decrease in HIV-1 infectivity (Fig. 6A and 6B), suggesting a different mechanism of Y2-mediated inhibitory effect on viral infection. Moreover, combined triple knockdown efficiently reduced endogenous levels of Y1-3 proteins in virus-producing cells (Fig. 6A, last lane), but only modestly increased HIV-1 infectivity (Fig. 6B), which are likely due to the different effects resulting from Y1/3 and Y2 knockdown.

To further investigate the role of Y1-3 proteins in HIV-1 production and infectivity, Y1-3 were transiently overexpressed in HEK293T cells to assess their effects on HIV-1 Gag protein expression and viral infectivity. Y1-3 overexpression did not significantly alter Gag protein levels in transfected cells, while intracellular p24 levels were reduced by 40-50% in Y1-3 overexpressing cells compared with vector-transfected control cells (Fig. 6C), suggesting that high levels of Y1-3 might negatively modulate proteolytic process of HIV-1 Gag. Consistently, Y1-3 overexpression decreased HIV-1 p24 levels in cell supernatants by 40-50% (data not shown). To evaluate the infectivity of viruses generated from Y1-3 overexpressing cells, viruses with equal amounts of p24 were used to infect TZM-bl indicator cells. The infectivity of HIV-1 generated from Y1-3 overexpressing cells was 40-50% lower compared with the virus generated from control cells (Fig. 6D), indicating negative effects of Y1-3 overexpression on HIV-1 production and viral infectivity.

274 **Y1-3 proteins and HIV-1 Gag form a complex with RNAs in cells**

275 To examine whether Y1-3 could interact with any HIV-1 proteins in cells, we performed
276 IP of overexpressed Y1-3 in HEK293T cells co-transfected with pNL4-3, and then detected HIV-
277 1 proteins in the input and IP products by immunoblotting using human anti-HIV-1
278 immunoglobulin (25). Interestingly, we found that Y1-3 co-precipitated with HIV-1 Gag (Pr55)
279 and intermediate Gag products, but not with HIV-1 p24 (Fig. 7, IP lanes). The vector cells were
280 used as a negative control for IP and showed a background band of Gag (Pr55) in the IP product
281 (Fig. 7, lane 2 from the left). Immunoblotting of FLAG confirmed expression and IP of FLAG-
282 tagged Y1-3 proteins in the transfected cells. Because both Y1-3 proteins and HIV-1 Gag can
283 bind cellular and HIV-1 RNAs (8, 10, 13, 26), to examine whether RNAs mediate the association
284 between Gag and Y1-3 proteins, cell lysates were treated with RNase A before IP. Interestingly,
285 RNase A treatment completely eliminated HIV-1 Gag signal in Y1-3 precipitation (Fig. 7, RNase
286 + IP lanes). These results suggest that Y1-3 proteins and HIV-1 Gag form a complex with RNAs
287 in cells.

288

289 **Inhibition of m^{6}A addition to HIV-1 RNA increases viral infectivity**

290 It has been shown that 3-deazaadenosine (DAA) blocks m^{6}A addition to mRNAs by
291 inhibiting the hydrolysis of S-adenosylhomocysteine, a competitive inhibitor of S-
292 adenosylmethionine, the methyl donor used by m^{6}A writers of the METTL3/14/WTAP complex
293 (27). Kennedy *et al.* showed that treatment of HIV-1 target CEM-SS cells with DAA (50 μM)
294 significantly reduces m^{6}A levels of cellular mRNA and inhibited the expression of HIV-1 Gag
295 and Nef proteins at 72 hpi without affecting cell viability and growth (12). They suggested that
296 drugs that reduce m^{6}A modification might have the potential to inhibit HIV-1 replication.

297 However, they did not test whether treatment of HIV-1-producing cells with DAA can reduce
298 m^{6}A levels of HIV-1 RNA, and thereby affect viral infectivity. To address these important
299 questions, we treated HEK293T cells with 50 μM DAA for 4 h before the transfection with the
300 HIV-1 proviral DNA construct (pNL4-3) to generate viruses. DAA concentration was
301 maintained for 48 h post-transfection before harvesting cells and HIV-1 for analyses. Compared
302 with the mock-treated cells as a control, DAA treatment did not affect cell viability and
303 proliferation (data not shown), but increased total HIV-1 Gag expression in cells by 4-fold (Fig.
304 8A). While the level of the Gag (Pr55) precursor was reduced, the levels of the processed p24
305 and intermediate Gag protein were largely increased in DAA treated cells relative to mock
306 treated cells (Fig. 8A), suggesting that DAA treatment of virus-producing cells may affect HIV-1
307 Gag processing. DAA treatment did not alter the levels of HIV-1 p24 in supernatants (Fig. 8B),
308 indicating that HIV-1 release from virus-producing cells was unaffected by DAA treatment. As
309 expected, the m^{6}A level of HIV-1 RNA derived from DAA-treated cells was 3-fold lower than
310 that from mock-treated cells (Fig. 8C). Interestingly, the infectivity of HIV-1 derived from DAA-
311 treated cells was 3-fold higher than that from mock-treated cells (Fig. 8D). These results suggest
312 that decreased m^{6}A modification of HIV-1 RNA could enhance viral infectivity, likely by
313 reducing the binding to Y1-3 proteins that have inhibitory effects on viral infection.
314

315 **Discussion**

316 Reversible m^{6}A modification is the most prevalent mRNA modification in eukaryotic organisms,
317 and plays critical roles in gene expression (5). Although m^{6}A modification was previously
318 identified in different viruses (28-30), its roles in HIV-1 gene expression regulation were
319 recently recognized (11-13). While these studies identified specific m^{6}A sites in HIV-1 gRNA,

320 they disagreed on the extent and locations of m^6A modifications along the HIV-1 genome and
321 their effects on viral replication (11-13). Lichinchi *et al.* (11) reported 14 peaks of m^6A
322 modification in HIV-1 RNA, in which the m^6A modification in the Rev response element region
323 increased binding to Rev and facilitated nuclear export of viral RNA, thereby enhancing HIV-1
324 replication. In contrast, Kennedy *et al.* (12) found 4 clusters of m^6A modification in the 3' UTR
325 region of HIV-1 RNA. Our study showed that HIV-1 gRNA has m^6A modifications in the 5' and
326 3' UTRs as well as *gag* and *rev* genes (13). Also, there is controversy regarding the roles of Y1-3
327 proteins in HIV-1 replication. In the presence of Y1-3 overexpression, Kennedy *et al*. observed
328 increased HIV-1 replication (12), while our data showed decreased HIV-1 replication (13). These
329 discrepancies could stem from different cell types or lines, reagents, and techniques used, and
330 need to be further investigated. In this study, we demonstrated that Y1-3 proteins suppress HIV-1
331 single-cycle and spreading infection in cells by decreasing viral gRNA and RT products. Y1-3
332 overexpression in HIV-1 infected cells led to significantly lower levels of early and late RT
333 product, and further decreased HIV-1 infectivity, suggesting that Y1-3 proteins could also inhibit
334 other steps after reverse transcription during the HIV-1 life cycle.

335 The GGACU is the predominant sequence in RRACH (R=G or A; H=A, C or U) motif
336 recognized by the m^6A writers (31). Our *in vitro* biochemical experiments reveal that Y1-3
337 proteins exhibit clear preference for the m^6A-modified HIV-1 RNA fragment over its unmodified
338 RNA counterpart. The preferential binding of m^6A sites in the HIV-1 genome to Y1-3 proteins
339 may contribute to decreased HIV-1 infection in HeLa/Y1-3 cells. There are two GGACU motifs
340 in the 5' UTR of HIV-1_{NL4-3} gRNA. The first GGACU motif is in the PBS region, and is
341 conserved in HIV-1 and simian immunodeficiency virus (SIV) (32), suggesting critical roles of
342 the motif in HIV-1 and SIV life cycles. The second GGACU motif is in the DIS stem. This motif

343 is conserved in HIV-1 subtype B isolates, but A to G mutations can be found in subtype C and
344 group O isolates (https://www.hiv.lanl.gov/).

345 Compared with WT viruses, mutant viruses harboring A to G mutations have
346 significantly reduced infectivity. We noted that the first GGACU motif is in the PBS and
347 mutation at this site in Mut 1/3 viruses (A to G at nt. 197) introduces a mismatch with $tRNA^{lys}$
348 primer (33), which may affect primer annealing and therefore impair viral infectivity. Recent
349 studies showed that the second GGACU motif interacts with HIV-1 nucleocapsid (NC) protein in
350 viral particles (33), and that nucleotides GGA in this motif strongly bind Gag precursor for viral
351 genome packaging (34). Mutation at this site may also impair interactions between HIV-1 gRNA
352 and NC protein, contributing to decreased infectivity in mutant viruses. Thus, the decreased
353 infectivity of Mut2 and Mut3 viruses (A to G at nt. 241) may be due to eliminated m^6A
354 modification at the second GGACU motif and/or decreased interactions between HIV-1 gRNA
355 and Gag/NC. The effects of these mutations on primer binding and Gag/NC interactions remain
356 to be examined.

357 Y1-3 proteins specifically recognizing m^6A sites via a hydrophobic pocket in the YTH
358 domain (3). The effects of Y1-3 on HIV-1 gene expression, viral production in virus-producing
359 HEK293T cells and infectivity of progeny HIV-1 appear complex. Individual or combined
360 knockdown of each endogenous Y1-3 decreased HIV-1 Gag expression in cells (Fig. 6A), while
361 overexpression of individual Y1-3 also decreased the levels of cell-associated p24 (Fig. 6C).
362 Knockdown of endogenous Y1 or Y3 increased progeny HIV-1 infectivity (Fig. 6B), while
363 overexpression of individual Y1-3 significantly decreased viral infectivity (Fig. 6D). The
364 complexity of these results might be due to broad effects of Y1-3 proteins on cellular gene
365 expression, which can in turn modulate HIV-1 gene expression, Gag processing, viral production

366 and infectivity. Furthermore, the m^{6}A modification regulates RNA processing and stability (2, 5,
367 35). After HIV-1 transcription, viral RNA undergoes extensive splicing to express structural and
368 accessory proteins. The roles of m^{6}A modification in HIV-1 RNA splicing, stability and
369 dimerization remain to be elucidated.

370 We demonstrated that HIV-1 Gag and Y1-3 proteins form a complex with RNAs in cells.
371 The association between Y1-3 proteins and HIV-1 Gag via cellular and/or viral RNA may
372 contribute to Y1-3-mediated inhibition of viral reverse transcription. We further show that
373 inhibition of m^{6}A addition to HIV-1 RNA by DAA treatment of virus-producing cells decreased
374 m^{6}A levels of HIV-1 RNA, but increases the infectivity of the derived viruses (Fig. 8). These
375 data suggest that reduced m^{6}A modification of HIV-1 RNA may decrease the binding to Y1-3
376 proteins, thereby relieving their inhibitory effects on viral infection.

377 In addition to HIV-1, recent studies have identified viral RNA m^{6}A modifications and its
378 roles in regulating replication of *Flaviviridae* viruses, including hepatitis C virus (HCV), dengue,
379 Zika virus (ZIKV), yellow fever virus, and West Nile virus (36, 37), Kaposi's sarcoma-
380 associated herpesvirus (KSHV) (38, 39), and influenza A virus (IAV) (40). The m^{6}A
381 modification in viral RNA increases RNA expression of IAV (40), promotes KSHV lytic
382 replication (38), but negatively regulates HCV and ZIKV production (36, 37). Similar to our
383 findings that Y1-3 proteins inhibit HIV-1 infection (13), Y1-3 proteins also negatively regulate
384 HCV and ZIKV replication (36, 37). A more recent study reported that Y2 protein negatively
385 regulates the KSHV lytic replication by enhancing decay of KSHV transcripts (39). Y1 and Y3
386 have no effect on IAV infection, while Y2 overexpression significant enhances IAV gene
387 expression and replication (40). Although different approaches in these studies may account for

388 discrepancies, these results suggest that m^{6}A modification and Y1-3 proteins have distinct effects
389 on various viruses.

390 The functional significance of viral RNA m^{6}A modifications remains to be established.
391 The innate immune system provides the first response to virus infections and to distinguish
392 between host and viral nucleic acids to mount protective antiviral immune responses. However,
393 viruses have developed different mechanisms to avoid innate immune recognition and antiviral
394 responses from the host. For example, Durbin *et al.* showed that the 106-nt polyU/UC sequence
395 derived from the 3' UTR of hepatitis C virus RNA triggers innate immune signaling after
396 binding to the retinoic acid-inducible gene I (RIG-I), an innate immune sensor for viral RNA.
397 Interestingly, the HCV RNA fragments containing m^{6}A or other modifications bind poorly to
398 RIG-I or fail to trigger RIG-I-mediated innate immune responses (41), suggesting that viral RNA
399 modifications could be an immune evasion strategy of viruses to avoid host antiviral responses.
400 It is conceivable that HIV-1 may exploit m^{6}A modifications of viral RNA to escape from innate
401 immunity to establish persistent infection, while Y1-3 proteins might act as a host defense
402 mechanism to partially counteract HIV-1 infection.

403 In summary, here we show that m^{6}A reader proteins Y1-3 inhibit HIV-1 infection by
404 decreasing viral gRNA and early reverse transcription products. We demonstrate that Y1-3
405 proteins preferentially bind to m^{6}A-modified HIV-1 RNA. Mutation of m^{6}A sites in the 5' UTR
406 resulted in decreased viral infectivity, suggesting important roles of these sites for HIV-1
407 infection. Y1-3 proteins and HIV-1 Gag form a complex with RNAs in virus-producing cells.
408 Furthermore, HIV-1 from virus-producing cells with decreased RNA m^{6}A levels enhances viral
409 infectivity, supporting the inhibitory effects of Y1-3 proteins on HIV-1 infection. Taken

410 together, these results help better understand the roles and mechanisms of m^6A modification of
411 HIV-1 RNA in regulating viral replication.
412
413 **Materials and Methods**
414 **Cell culture**. HEK293T cell line (a kind gift from Dr. Vineet KewalRamani, National Cancer
415 Institute, Frederick, USA) and TZM-bl cells [(23) obtained through the NIH AIDS Reagent
416 Program, Catalog # 8129] were maintained in complete DMEM as described (42). HeLa or
417 HeLa/CD4 cell lines (kind gifts from Dr. Vineet KewalRamani, National Cancer Institute,
418 Frederick, USA) overexpressing empty vector (pPB-CAG), individual FLAG- and HA-tagged
419 Y1, Y2 or Y3 protein were maintained in complete DMEM containing 2 μg/ml puromycin as
420 described (13).
421
422 **Generating HeLa cell lines stably express CD4 and Y1-3 proteins.** HeLa/CD4 cells were
423 generated by transduction of HeLa cells with a pMX retroviral vector expressing human CD4
424 (43). HeLa/CD4 cells were transfected separately with pPB-CAG vector-based Y1-3 expressing
425 constructs or pPB-CAG empty vector, and then selected with puromycin (2 μg/ml). HeLa/CD4
426 stably expressing cells Y1-3 were cultured as described (13).
427
428 **Mutagenesis in HIV-1 proviral DNA plasmid (pNL4-3).** Mutations in pNL4-3 were
429 introduced using Agilent QuickChange Lightning Multi Site-directed Mutagenesis Kit (catalog #
430 210515-5) according to the instructions. Primers mut1 (5'-CCCGAACAGGGGCTTGAAAGC-
431 3') and mut2 (5'-TCGACGCAGGGCTCGGCTTG-3') were used (mutation sites are underlined)

to generate A to G mutation at the first (nt. 197), the second (nt. 241) or both GGACU motifs between HIV-1 gRNA U5 and *gag* gene. The mutations were confirmed by DNA sequencing.

siRNA knockdown of Y1-3 proteins. Y1-3 expressions were knocked down by two rounds of siRNA transfection using specific siRNAs (QIAGEN) and Lipofectamine RNAiMax (Invitrogen) according to instructions (siRNA sequences are listed in Table 1). Briefly, HEK293T cells (1.5×10^5 per well) in 24-well plates were transfected with gene specific siRNAs or control siRNA. Twenty-four h after transfection, cell culture media were replaced and the second-round siRNA transfection was conducted. At 6 h after the second round of siRNA transfection, pNL4-3 (0.5 μg per well) was transfected to HEK293T cells. Cells and culture media were collected at 36 h after pNL4-3 transfection for immunoblotting, p24 quantification, and infection assays.

HIV-1 stocks and infection assays. Single-cycle HIV-luc/VSV-G was generated as previously described (13). Replication-competent WT and mutant HIV-1 stocks were generated by transfection of HEK293T cells with pNL4-3 or mutant proviral DNA plasmids using Lipofectamine 2000 (Invitrogen) according to instructions. For Y1-3 and pNL4-3 co-expression experiments, pPB-CAG vector or pPB-CAG expressing individual FLAG- and HA- tagged Y1-3 protein was transfected into HEK293T cells, and pNL4-3 proviral DNA was transfected 12 h later. At 48 h (WT and Mut1-3 plasmids) or 36 h (Y1-3 co-expression) after proviral DNA transfection, cells were collected for immunoblotting and HIV-1 capsid p24 levels in viral stocks were quantified by an enzyme-linked immunosorbent assay (ELISA) using anti-p24-coated plates (AIDS and Cancer Virus Program, NCI-Frederick, MD) as described (13, 43). To compare

infectivity of WT HIV-1 in HeLa/Y1-3 cells, HIV-luc/VSV-G was used for infection at multiplicity of infection (MOI) at 1 as described (13). To compare the infectivity of WT HIV-1_{NL4-3} and mutant viruses, viruses with equal amounts of p24 (400 pg) were used to infect TZM-bl cells in 24-well plates. At 48 hpi, TZM-bl cells were washed twice with PBS and lysed for luciferase assay (Promega) according to the manufacturer's instructions. Cell protein concentrations were quantified using a bicinchoninic acid assay (Pierce) and all luciferase results were normalized based on total protein input.

Flow cytometry measure cell surface levels of CD4 and CXCR4. HeLa/CD4 cells were treated with the non-enzymatic cell dissociation solution (C5914, Sigma-Aldrich) and double stained with FITC-conjugated CD4 (MHCCD0401-4, Thermo Fisher) and phycoerythrin-conjugated CXCR4 (555974, BD Pharmingen) antibodies as described (13). Cells stained with a mouse IgG2a isotype antibody (555574, BD Pharmingen) were used as a negative control. Flow cytometry was analyzed using a Guava EasyCyte Mini and data analysis was performed using FlowJo (FlowJo, LLC) software as described (44).

IP of Y1-3 proteins and RT-qPCR detection of HIV-1 gRNA. HeLa/CD4 cells expressing MAL were generated by transfection with pEF-Bos MAL Flag (plasmid # 41554 from Addgene) (17). HeLa/CD4 cells expressing pPB-CAG vector, MAL or Y1-3 proteins (3×10^6 cells) were seeded in a 60 mm-diameter culture plate one day before HIV-1 infection. Cells were infected with HIV-1_{NL4-3} at a multiplicity (MOI) of infection of 5 for 3 h. Cells were UV-cross-linked and lysed in cell lysis buffer (Sigma-Aldrich). Co-immunoprecipitated RNA was isolated and RT-qPCR quantification of HIV-1 gRNA was performed as described (13).

Antibodies and immunoblotting. Antibodies used in this study were: anti-GAPDH (clone 4G5, AbD serotec, Atlanta, GA), anti-FLAG (F-3165, Sigma-Aldrich), anti-YTHDF1 (ab99080, Abcam), anti-YTHDF2 (ABE542, EMD Millipore, Billerica, MA), anti-YTHDF3 (ab103328, Abcam), and anti-HIV-1 p24 (AIDS Reagent Program, catalog # 6458). Cells were harvested and lysed in cell lysis buffer (Cell Signaling, Beverly, MA) supplemented with the protease inhibitor cocktail (Sigma-Aldrich). Immunoblotting was performed and ImageJ software (NIH) was used to calculate the densitometry of immunoblotting bands as described (13).

AlphaScreen assay. Recombinant glutathione-S-transferase (GST)-tagged Y1-3 proteins were purified as described (8). Two RNA fragments, control RNA and m^6A-modified RNA (m^6A RNA), corresponding to 235-281 nt containing the second GGACU consensus sequence, were synthesized (Integrated DNA Technologies), and the RNA fragments were modified with biotin at both 5' and 3' ends. Control RNA has no m^6A modification, while m^6A RNA fragment has m^6A modification in GGACU motif. To eliminate RNA dimerization, the DIS sequence (AAGCGCGC) was substituted with nucleotides GAG as described in a previous study (45). AlphaScreen assays were conducted as previously reported with minor modifications (20). Proteins and RNA fragments were diluted with AlphaScreen buffer (100 mM NaCl, 1 mM $MgCl_2$, 1 mM DTT, 1 mg/mL BSA, 25 mM Tris pH 7.5). For the binding of proteins and acceptor beads, Y1-3 proteins (25 nM) and acceptor beads (catalog # AL110C, 1:100 dilution; PerkinElmer) were mixed and adjusted to 30 µL, and incubated at 4 °C for 2 h. For RNA and donor bead binding, control or m^6A RNA (50 nM) were mixed with donor beads (catalog # 6760002S, 1:100 dilution; PerkinElmer) in 10 µL volume, and incubated at 4 °C for 2 h. After

the incubation, the protein and RNA were mixed, and incubated at 4 °C for 1 h. Samples (25 µL) were added to microplate and read with EnSpire multimode plate reader (PerkinElmer).

***In vitro* pull-down assays for RNA and Y1-3 protein binding.** Streptavidin Dynabeads M-280 (Invitrogen, catalog # 11205D) was used in this experiment. Beads were washed and incubated with biotin-labeled m^{6}A RNA or control RNA at 4 °C for 60 min according to the manufacturer's instructions, and purified Y1-3 proteins were added at concentrations of 1, 5, 25, 125, and 625 nM and incubated for 60 min. After washing, proteins bound to beads were eluted for immunoblotting using specific antibodies to Y1, Y2, or Y3.

qPCR assays. To quantify HIV-1 gRNA after infection of HeLa/Y1-3 cells, at 1, 3 and 6 h after viral infection, cells were collected and total RNAs were extracted with an RNeasy Mini kit (Qiagen). Reverse transcription was conducted with first-strand synthesis (Invitrogen). qPCR was used to measure HIV-1 gRNA as described (46). To quantify HIV-1 early and late RT products after viral infection, cellular DNA was extracted using a QIAamp DNA Blood Mini kit (Qiagen). Early RT products were quantified using primers ert2f (5'-GTGCCC GTCTGTTGTGTGAC-3') and ert2r (5'-GGCGCCACTGCTAGAGATTT-3'). Late RT products were quantified using primers LW59 and LW60 as described (13). GAPDH levels were also quantified to normalize early and late RT data (13).

IP of Y1-3 proteins to detect the interactions with HIV-1 proteins. HEK293T cells (1×10^6) were co-transfected with 2 µg pNL4-3 and 2 µg empty vector (pPB-CAG) or constructs expressing individual HA-tagged Y1-3 proteins as previously described (13). At 48 h post-

transfection, cells were harvested, lysed in 1% digitonin and total protein concentration was quantified. To elucidate the effects of RNAs in Gag and Y1-3 interactions, one aliquot of each cell lysate was treated with RNase A (100 µg/ml) for 1 h at room temperature, and IP was conducted as described (47). Proteins bound to anti-HA agarose beads were eluted by boiling in sample buffer for immunoblotting. HIV Immunoglobulin (HIV-IG, NIH AIDS Reagent Program, catalog # 3957) (25) was used to detect HIV-1 proteins precipitated by Y1-3 proteins.

Prediction of the secondary structure of HIV-1 RNA segments. The secondary RNA structures of HIV-1 5'UTR segments from WT HIV-1 or mutants were predicted using online mfold program according to the user's instruction (http://unafold.rna.albany.edu/?q=mfold).

Generation of m^{6}A-reduced HIV-1 from cells treated with DAA. HEK293T cells were mock treated with mock or 50 µM DAA (Sigma-Aldrich, Product number D8296) for 4 h before transfection with pNL4-3 plasmid as described (12, 13). DAA concentration (50 µM) was maintained in the culture medium for additional 48 h. Cells and supernatants were collected at 48 h post-transfection for the analysis of protein expression and RNA m^{6}A by immunoblotting.

Immunoblot analysis of m^{6}A of HIV-1 RNA. HIV-1 RNA was extracted from HIV-1 generated from mock- or DAA-treated HEK293T cells with an RNA purification kit (Qiagen) as described (13). HIV-1 RNA (50 ng/sample) was used for m^{6}A dot blotting with rabbit polyclonal anti-m^{6}A antibodies (Synaptic Systems; Cat # 202 003) as previously described (11, 12). Densitometric quantification of the m^{6}A signal intensity was performed using ImageJ software (NIH).

Statistical analyses. Mann Whitney test was used to analyze AlphaScreen signal for m^6A and control RNA fragment binding to Y1-3 proteins (Fig. 4C). Dunnett's multiple comparison test was used for statistical analysis of all other data as indicated in figure legends. $P < 0.05$ is considered significant.

Acknowledgments

This work was supported by a grant (GM128212) from the National Institutes of Health (NIH) to L.W. L.W. was also supported in part by NIH grants (AI120209 and AI104483). M.K. was supported by NIH grant AI062520. The funders had no role in study design, data collection and analysis, decision to publish, or preparation of the manuscript. We thank Dr. Vineet KewalRamani for sharing reagents, Dr. Corine St. Gelais for critical reading the manuscript, and the Wu lab members for valuable discussions. The following reagents were obtained through the NIH AIDS Reagent Program, Division of AIDS, NIAID, NIH: HIV-1 p24 Gag Monoclonal (#24-3) from Dr. Michael H. Malim; HIV-IG (catalog #3957) from NABI and NHLBI; TZM-bl from Dr. John C. Kappes, Dr. Xiaoyun Wu and Tranzyme Inc.

Author contributions

Conceived and designed the experiments: WL, NT, MK, LW. Performed the experiments: WL, NT, PCK. Analyzed the data: WL, NT, PCK, MK, CH, LW. Provided key reagents (purified recombinant Y1-3 proteins): CL. Wrote the paper: WL, NT, MK, LW.

570 **References**

571 1. Wei CM, Gershowitz A, Moss B. Methylated nucleotides block 5' terminus of HeLa cell
572 messenger RNA. Cell. 1975;4(4):379-86.

573 2. Roundtree IA, Evans ME, Pan T, He C. Dynamic RNA Modifications in Gene
574 Expression Regulation. Cell. 2017;169(7):1187-200.

575 3. Li F, Zhao D, Wu J, Shi Y. Structure of the YTH domain of human YTHDF2 in complex
576 with an m(6)A mononucleotide reveals an aromatic cage for m(6)A recognition. Cell Res.
577 2014;24(12):1490-2.

578 4. Meyer KD, Jaffrey SR. The dynamic epitranscriptome: N6-methyladenosine and gene
579 expression control. Nat Rev Mol Cell Biol. 2014;15(5):313-26.

580 5. Fu Y, Dominissini D, Rechavi G, He C. Gene expression regulation mediated through
581 reversible m(6)A RNA methylation. Nat Rev Genet. 2014;15(5):293-306.

582 6. Sheth U, Parker R. Decapping and decay of messenger RNA occur in cytoplasmic
583 processing bodies. Science. 2003;300(5620):805-8.

584 7. Meyer KD, Saletore Y, Zumbo P, Elemento O, Mason CE, Jaffrey SR. Comprehensive
585 analysis of mRNA methylation reveals enrichment in 3' UTRs and near stop codons. Cell.
586 2012;149(7):1635-46.

587 8. Wang X, Lu Z, Gomez A, Hon GC, Yue Y, Han D, et al. N6-methyladenosine-dependent
588 regulation of messenger RNA stability. Nature. 2014;505(7481):117-20.

589 9. Meyer KD, Patil DP, Zhou J, Zinoviev A, Skabkin MA, Elemento O, et al. 5' UTR m(6)A
590 Promotes Cap-Independent Translation. Cell. 2015;163(4):999-1010.

591 10. Shi H, Wang X, Lu Z, Zhao BS, Ma H, Hsu PJ, et al. YTHDF3 facilitates translation and
592 decay of N6-methyladenosine-modified RNA. Cell Res. 2017;27(3):315-28.

593 11. Lichinchi G, Gao S, Saletore Y, Gonzalez GM, Bansal V, Wang Y, et al. Dynamics of
594 the human and viral m(6)A RNA methylomes during HIV-1 infection of T cells. Nat Microbiol.
595 2016;1:16011.

596 12. Kennedy EM, Bogerd HP, Kornepati AV, Kang D, Ghoshal D, Marshall JB, et al.
597 Posttranscriptional m(6)A Editing of HIV-1 mRNAs Enhances Viral Gene Expression. Cell Host
598 Microbe. 2016;19(5):675-85.

599 13. Tirumuru N, Zhao BS, Lu W, Lu Z, He C, Wu L. N(6)-methyladenosine of HIV-1 RNA
600 regulates viral infection and HIV-1 Gag protein expression. Elife. 2016;5.

601 14. Antonucci JM, St Gelais C, de Silva S, Yount JS, Tang C, Ji X, et al. SAMHD1-mediated
602 HIV-1 restriction in cells does not involve ribonuclease activity. Nat Med. 2016;22(10):1072-4.

603 15. St Gelais C, Roger J, Wu L. Non-POU Domain-Containing Octamer-Binding Protein
604 Negatively Regulates HIV-1 Infection in CD4(+) T Cells. AIDS Res Hum Retroviruses.
605 2015;31(8):806-16.

606 16. Fitzgerald KA, Palsson-McDermott EM, Bowie AG, Jefferies CA, Mansell AS, Brady G,
607 et al. Mal (MyD88-adapter-like) is required for Toll-like receptor-4 signal transduction. Nature.
608 2001;413(6851):78-83.

609 17. Fitzgerald KA, McWhirter SM, Faia KL, Rowe DC, Latz E, Golenbock DT, et al.
610 IKKepsilon and TBK1 are essential components of the IRF3 signaling pathway. Nat Immunol.
611 2003;4(5):491-6.

612 18. Wei CM, Moss B. Nucleotide sequences at the N6-methyladenosine sites of HeLa cell
613 messenger ribonucleic acid. Biochemistry. 1977;16(8):1672-6.

614 19. Dominissini D, Moshitch-Moshkovitz S, Schwartz S, Salmon-Divon M, Ungar L,
615 Osenberg S, et al. Topology of the human and mouse m6A RNA methylomes revealed by m6A-
616 seq. Nature. 2012;485(7397):201-6.

617 20. Kessl JJ, Kutluay SB, Townsend D, Rebensburg S, Slaughter A, Larue RC, et al. HIV-1
618 Integrase Binds the Viral RNA Genome and Is Essential during Virion Morphogenesis. Cell.
619 2016;166(5):1257-68 e12.

620 21. Telesnitsky A, Wolin SL. The Host RNAs in Retroviral Particles. Viruses. 2016;8(8).

621 22. Eckwahl MJ, Telesnitsky A, Wolin SL. Host RNA Packaging by Retroviruses: A Newly
622 Synthesized Story. MBio. 2016;7(1):e02025-15.

623 23. Derdeyn CA, Decker JM, Sfakianos JN, Wu X, O'Brien WA, Ratner L, et al. Sensitivity
624 of human immunodeficiency virus type 1 to the fusion inhibitor T-20 is modulated by coreceptor
625 specificity defined by the V3 loop of gp120. J Virol. 2000;74(18):8358-67.

626 24. Kharytonchyk S, Monti S, Smaldino PJ, Van V, Bolden NC, Brown JD, et al.
627 Transcriptional start site heterogeneity modulates the structure and function of the HIV-1
628 genome. Proc Natl Acad Sci U S A. 2016;113(47):13378-83.

629 25. Cummins LM, Weinhold KJ, Matthews TJ, Langlois AJ, Perno CF, Condie RM, et al.
630 Preparation and characterization of an intravenous solution of IgG from human
631 immunodeficiency virus-seropositive donors. Blood. 1991;77(5):1111-7.

632 26. Kutluay SB, Zang T, Blanco-Melo D, Powell C, Jannain D, Errando M, et al. Global
633 changes in the RNA binding specificity of HIV-1 gag regulate virion genesis. Cell.
634 2014;159(5):1096-109.

635 27. Chiang PK. Biological effects of inhibitors of S-adenosylhomocysteine hydrolase.
636 Pharmacol Ther. 1998;77(2):115-34.

637 28. Krug RM, Morgan MA, Shatkin AJ. Influenza viral mRNA contains internal N6-
638 methyladenosine and 5'-terminal 7-methylguanosine in cap structures. J Virol. 1976;20(1):45-53.

639 29. Beemon K, Keith J. Localization of N6-methyladenosine in the Rous sarcoma virus
640 genome. J Mol Biol. 1977;113(1):165-79.

641 30. Canaani D, Kahana C, Lavi S, Groner Y. Identification and mapping of N6-
642 methyladenosine containing sequences in simian virus 40 RNA. Nucleic Acids Res.
643 1979;6(8):2879-99.

644 31. Ping XL, Sun BF, Wang L, Xiao W, Yang X, Wang WJ, et al. Mammalian WTAP is a
645 regulatory subunit of the RNA N6-methyladenosine methyltransferase. Cell Res.
646 2014;24(2):177-89.

647 32. Pollom E, Dang KK, Potter EL, Gorelick RJ, Burch CL, Weeks KM, et al. Comparison of
648 SIV and HIV-1 genomic RNA structures reveals impact of sequence evolution on conserved and
649 non-conserved structural motifs. PLoS Pathog. 2013;9(4):e1003294.

650 33. Wilkinson KA, Gorelick RJ, Vasa SM, Guex N, Rein A, Mathews DH, et al. High-
651 throughput SHAPE analysis reveals structures in HIV-1 genomic RNA strongly conserved
652 across distinct biological states. PLoS Biol. 2008;6(4):e96.

653 34. Abd El-Wahab EW, Smyth RP, Mailler E, Bernacchi S, Vivet-Boudou V, Hijnen M, et
654 al. Specific recognition of the HIV-1 genomic RNA by the Gag precursor. Nat Commun.
655 2014;5:4304.

656 35. Liu N, Dai Q, Zheng G, He C, Parisien M, Pan T. N(6)-methyladenosine-dependent RNA
657 structural switches regulate RNA-protein interactions. Nature. 2015;518(7540):560-4.

658 36. Gokhale NS, McIntyre AB, McFadden MJ, Roder AE, Kennedy EM, Gandara JA, et al.
659 N6-Methyladenosine in Flaviviridae Viral RNA Genomes Regulates Infection. Cell Host
660 Microbe. 2016;20(5):654-65.

661 37. Lichinchi G, Zhao BS, Wu Y, Lu Z, Qin Y, He C, et al. Dynamics of Human and Viral
662 RNA Methylation during Zika Virus Infection. Cell Host Microbe. 2016;20(5):666-73.

663 38. Ye F, Chen ER, Nilsen TW. Kaposi's Sarcoma-Associated Herpesvirus Utilizes and
664 Manipulates RNA N6-Adenosine Methylation To Promote Lytic Replication. J Virol.
665 2017;91(16):e00466-17.

666 39. Tan B, Liu H, Zhang S, da Silva SR, Zhang L, Meng J, et al. Viral and cellular N(6)-
667 methyladenosine and N(6),2'-O-dimethyladenosine epitranscriptomes in the KSHV life cycle.
668 Nat Microbiol. 2018;3(1):108-20.

669 40. Courtney DG, Kennedy EM, Dumm RE, Bogerd HP, Tsai K, Heaton NS, et al.
670 Epitranscriptomic Enhancement of Influenza A Virus Gene Expression and Replication. Cell
671 Host Microbe. 2017;22(3):377-86.

672 41. Durbin AF, Wang C, Marcotrigiano J, Gehrke L. RNAs Containing Modified
673 Nucleotides Fail To Trigger RIG-I Conformational Changes for Innate Immune Signaling.
674 MBio. 2016;7(5).

675 42. Dong C, Kwas C, Wu L. Transcriptional restriction of human immunodeficiency virus
676 type 1 gene expression in undifferentiated primary monocytes. J Virol. 2009;83(8):3518-27.

677 43. Wang JH, Janas AM, Olson WJ, KewalRamani VN, Wu L. CD4 coexpression regulates
678 DC-SIGN-mediated transmission of human immunodeficiency virus type 1. J Virol.
679 2007;81(5):2497-507.

680 44. Wang JH, Kwas C, Wu L. Intercellular adhesion molecule 1 (ICAM-1), but not ICAM-2
681 and -3, is important for dendritic cell-mediated human immunodeficiency virus type 1
682 transmission. J Virol. 2009;83(9):4195-204.

683 45. Keane SC, Heng X, Lu K, Kharytonchyk S, Ramakrishnan V, Carter G, et al. Structure of
684 the HIV-1 RNA packaging signal. Science. 2015;348(6237):917-21.

685 46. Dong C, Janas AM, Wang JH, Olson WJ, Wu L. Characterization of human
686 immunodeficiency virus type 1 replication in immature and mature dendritic cells reveals
687 dissociable cis- and trans-infection. J Virol. 2007;81(20):11352-62.

688 47. St Gelais C, de Silva S, Hach JC, White TE, Diaz-Griffero F, Yount JS, et al.
689 Identification of cellular proteins interacting with the retroviral restriction factor SAMHD1. J
690 Virol. 2014;88(10):5834-44.

691

692 **Figure Legends**

693

694 **Fig 1. Overexpression of Y1-3 proteins inhibits postentry HIV-1 infection through**

695 **decreasing HIV-1 genomic RNA (gRNA) and inhibiting viral reverse transcription (RT).**

696 (**A**) Overexpression of Y1-3 proteins in HeLa/Y1-3 cell lines. (**B**) Cells were infected with HIV-

697 1 Luc/VSV-G (MOI=1), and viral infection was measured by luciferase activity at 24 h post-

698 infection (hpi) (n=3 independent experiments, same in the following). (**C**) Quantified HIV-1

699 gRNA levels after infection of HeLa/Y1-3 cells and vector control cells (n=3). (**D**) Early RT

700 product levels at 6, 12 and 24 hpi (n=3). (**E**) Late RT product levels at 6, 12 and 24 hpi (n=3).

701 Results are shown as mean ± SEM. Dunnett's multiple comparison test was used to determine

statistical significance. * $P < 0.05$, *** $P < 0.0005$, compared each group with vector control cells in each corresponding experiment. Data are from at least 3 independent experiments with biological duplicates.

Fig 2. **Overexpression of reader proteins YTHDF1-3 (Y1-3) in HeLa/CD4 cells inhibits wild-type HIV-1 replication. (A)** Surface levels of CD4 (exogenous) and CXCR4 (endogenous) in HeLa/CD4 cells overexpressing individual Y1-3 proteins or vector control cells were analyzed by flow cytometry. Isotype-matched IgG was used as a negative control for immunostaining. The numbers on the top of the plots indicate the percentages of CD4- and CXCR4-positive cells. (**B**) HeLa/CD4 cells overexpressing individual Y1-3 proteins were infected with HIV-1_{NL4-3} (MOI=1) for 72 h. HIV-1 Gag protein expression and over-expression of FLAG-tagged Y1-3 proteins in HeLa/CD4 cells were confirmed by immunoblotting. (**C**) ELISA quantification of HIV-1 p24 levels in the supernatants from infected cells. (**D** and **E**) qPCR quantification of the levels of HIV-1 early RT products (D) and late RT products (E). (**F**) RT-qPCR quantification of HIV-1 *gag* mRNA in the cells. (C-F) The reverse transcriptase inhibitor nevirapine (NVP) was used to treat vector cells as a negative control for HIV-1 infection. All results are shown as mean ± SEM (n=3) and data presented are representative of 3 independent experiments. Dunnett's multiple comparison test was used to determine statistical significance. ** $P < 0.005$ and *** $P < 0.0005$ compared with vector control cells.

Fig 3. YTHDF1-3 proteins bind to wild-type HIV-1 gRNA in infected HeLa/CD4 cells. (A) Immunoblotting of Y1-3 in the input and immunoprecipitation (IP) samples from HeLa/CD4 cells infected with HIV-1. HeLa/CD4 cells stably overexpressing FLAG-tagged Y1-3 proteins,

MAL (MyD88 adapter-like protein), or empty vector control cells were infected with HIV-1_{NL4-3} at an MOI of 5 for 3 h. FLAG antibodies were used to immunoprecipitate Y1-3 proteins or MAL in HeLa/CD4 cells after HIV-1 infection. **(B)** HIV-1 gRNA is bound by Y1-3 proteins expressed in HeLa/CD4 cells. HIV-1 infection of HeLa/CD4 cells overexpressing Y1-3 proteins, MAL, or empty vector control cells as described above in (A). Cell lysates were immunoprecipitated with anti-FLAG antibody, and HIV-1 *gag* RNA levels were quantified by RT-qPCR. Dunnett's multiple comparison test was used to determine statistical significance. *** $P < 0.0005$ compared with the vector control cells. Data presented are representative of 4 independent experiments.

Fig 4. **Y1-3 proteins preferentially bind to an m^{6}A-modifed HIV-1 RNA fragment *in vitro*.** **(A)** Structure of partial HIV-1 RNA 5' UTR containing two GGACU motifs (in gray background) that are labeled with blue words *m^{6}A #1* (nt. 195-199) and *m^{6}A #2* (nt. 239-243). PBS and DIS are highlighted in bold. The figure is adapted from Kharytonchyk et al. (24). **(B)** Sequences of synthesized control (Ctrl) RNA and m^{6}A-modified (m^{6}A RNA) fragment containing the second GGACU motif (in bold) in HIV-1 RNA 5' UTR corresponding to nt. 235-281. The DIS-containing sequence (AA**GCGCGC**) was replaced with nucleotides GAG (underlined) to eliminate RNA dimerization. The A* indicates the m^{6}A modification site in the RNA fragment. **(C)** Binding of Y1-3 proteins to m^{6}A RNA versus control, unmodified RNA was monitored using the AlphaScreen assay. Data are from two independent experiments with biological triplicates. Results are shown as mean ±SEM. ** $P < 0.005$ by Mann Whitney test. **(D)** Y1-3 protein pull-down using biotin-labeled control and m^{6}A RNA fragments. Streptavidin Dynabeads were used in the pull-down assay and immunoblotting was performed using specific antibodies to Y1, Y2, or Y3. **(E)** Y1-3 protein pull-down level based on densitometry analysis of

748 the bands in immunoblotting. Data are average results from two independent experiments. (**F**)
749 Calculated concentrations of Y1-3 proteins needed to reach 50% pull-down levels of 625 nM
750 Y1-3 by the m^6A RNA fragment.
751
752 **Fig 5. A to G mutations in GGACU motifs of the 5' UTR of HIV-1 gRNA reduce viral**
753 **infectivity.** (**A)** Schematic representation of introduced mutations in the 5' UTR region of HIV-1
754 proviral DNA. (**B)** Gag protein expression in HEK293T cell lysates expressing wild type (WT)
755 and mutants (Mut1-3). The relative p24 levels were normalized based on GAPDH levels. **(C)**
756 HIV-1 p24 levels in the supernatants at 48 h post-transfection were quantified by ELISA (n=3).
757 **(D)** Infectivity of WT and mutant HIV-1 was quantified by measuring luciferase activity 48 h
758 after infection of TZM-bl cells (n=4). Results are shown as mean ±SEM. Dunnett's multiple
759 comparison test was used for statistical analysis. *** $P < 0.0005$, compared HIV-1 mutants to
760 WT virus. **(E)** Endogenous Y1-3 proteins in TZM-bl cells were knocked down by combined Y1-
761 3 specific siRNA transfection. Immunoblotting confirms Y1-3 knockdown compared to control
762 siRNA-transfected cells. **(F)** The infectivity of WT and mutant HIV-1 was quantified by
763 measuring luciferase activity 48 h after infection of TZM-bl cells (n=4). Results are shown as
764 mean ±SEM. Dunnett's multiple comparison test was used for statistical analysis. * $P<0.05$,
765 compared HIV-1 mutants with WT HIV-1. **(G)** Predicted secondary structures of the RNA
766 segments containing the PBS (left two panels) or DIS (right two panels, sequences are
767 highlighted in bold) of WT, Mut1 and Mut2 viruses. Two A to G mutation sites (Mut1 and
768 Mut2) are circled and pointed by blue arrows.
769

Fig 6. Effects of Y1-3 knockdown or overexpression in virus-producing cells on HIV-1 Gag expression and viral infectivity. (A and **B)** HEK293T cells were transfected with non-specific control siRNA or siRNA specific for Y1-3 (individual or combined), and 24 h later, the cells were transfected with siRNA as above described for second round. At 6 h after the second round of siRNA transfection, cells were transfected with pNL4-3. Cells and culture media were collected at 36 h after pNL4-3 transfection for immunoblotting and infection assays. **(A)** Immunoblotting of HIV-1 Gag and endogenous Y1-3 in HEK293T cells with single or triple Y1-3 knockdown and pNL4-3 transfection. GAPDH was a loading control. **(B)** Infectivity of equal amounts of HIV-1 (400 pg p24) generated in control cells, or cells with individual or triple Y1-3 knockdown was quantified by measuring luciferase activity 48 h after infection of TZM-bl cells (n=3). Results are shown as mean ± SEM. Dunnett's multiple comparison tests were used for statistical analysis. ** $P < 0.005$, *** $P < 0.0005$, compared Y1-3 specific siRNA knockdown with non-specific control (Ctrl) siRNA. **(C** and **D)** HEK293T cells were transfected separately with Y1-3 expressing plasmids or empty vector, and 12 h later, cells were transfected with pNL4-3. **(C)** Immunoblotting of HIV-1 Gag and FLAG-tagged Y1-3 in cells collected at 36 h post pNL4-3 transfection. GAPDH was a loading control. **(D)** Infectivity of equal amounts of HIV-1 (400 pg p24) was quantified by measuring luciferase activity 48 h after infection of TZM-bl cells (n=3). Results are shown as mean ±SEM. Dunnett's multiple comparison test was used for statistical analysis. ** $P <0.005$, *** $P < 0.0005$, compared Y1-3 overexpression with vector controls.

Fig 7. Y1-3 proteins and HIV-1 Gag form a complex with RNAs in cells. HEK293T cells were co-transfected with pNL4-3 and individual plasmids expressing HA- and FLAG-tagged

Y1-3 or empty vector. Cell lysates were treated with or without RNase A (100 µg/ml) before immunoprecipatation (IP) of Y1-3 proteins using anti-HA agarose beads. The input or IP products of HIV-1 Gag or CA (p24) were detected using HIV Immunoglobulin. Expression and IP of Y1-3 were confirmed with anti-FLAG immunoblotting. Results presented are representative of three independent experiments.

Fig 8. Inhibition of m^{6}A addition to HIV-1 RNA increases viral infectivity. HEK293T cells were pretreated with 50 µM 3-deazadenine (DAA) or mock treated for 4 h and transfected with pNL4-3 plasmid DNA. At 48 h post-transfection, cells and supernatant were collected for analyses. **(A)** Cell lysates were analyzed for HIV-1 Gag expression. GAPDH was a loading control. Relative levels of HIV-1 total Gag normalized to GAPDH levels are shown. **(B)** HIV-1 p24 levels in the supernatant of transfected HEK293T cells were measured by ELISA. **(C)** RNA (50 ng/sample) extracted from HIV-1 generated from the mock- or DAA-treated HEK293T cells were used to measure m^{6}A levels using a dot-blot assay. The m^{6}A dot intensity was quantified by densitometry. **(D)** Equal amounts of HIV-1 (p24 of 500 pg or 1,000 pg) were used to infect TZM-bl cells to analyze viral infectivity at 24 hpi. The value of HIV-1 from mock-treated cells (500 pg HIV-1 input) was set as 100%. Relative infectivity is shown and results are shown as mean ±SEM. Dunnett's multiple comparison tests were used for statistical analysis. * $P < 0.05$, *** $P < 0.0005$, compared mock-treated control with 500 pg of HIV-1 input. Results presented are representative of two independent experiments.

813 **Table 1. Sequences of siRNAs used for Y1-3 knockdown**

Targets	**Catalog numbers (QIAGEN)**	**Target sequences (5'- 3')**
YTHDF1	SI00764715	CCGCGTCTAGTTGTTCATGAA
YTHDF1	SI04240117	CCCTCCACCCATAAAGCATAA
YTHDF1	SI04240418	TACGGACAGCTCAGTAACGGA
YTHDF1	SI04279121	CAGGCTGGAGAATAACGACAA
YTHDF2	SI00764757	AAGGACGTTCCCAATAGCCAA
YTHDF2	SI04270777	TTCGGTCCATTAATAACTATA
YTHDF3	SI00764778	ATGGATTAAATCAGTATCTAA
YTHDF3	SI04133339	TAAGTCAAAGAAGACGTATTA
Negative Control	SI03650325	AATTCTCCGAACGTGTCACGT

814

Fig. 1

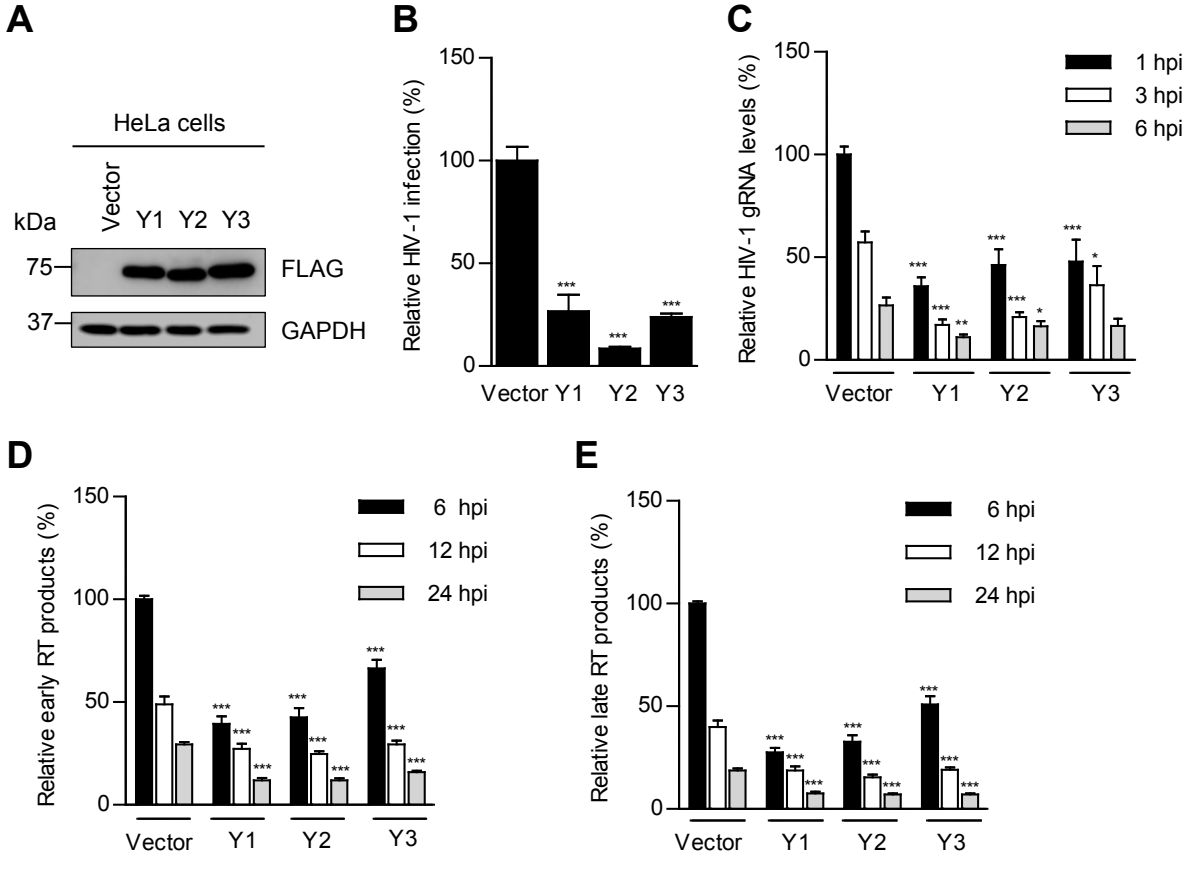
A
HeLa cells
Vector
Y1
Y2
Y3
kDa
75
37
FLAG
GAPDH
B
Relative HIV-1 infection (%)
150
100
50
0
Vector
Y1
Y2
Y3
C
Relative HIV-1 gRNA levels (%)
1 hpi
3 hpi
6 hpi
D
Relative early RT products (%)
6 hpi
12 hpi
24 hpi
E
Relative late RT products (%)

Fig. 2

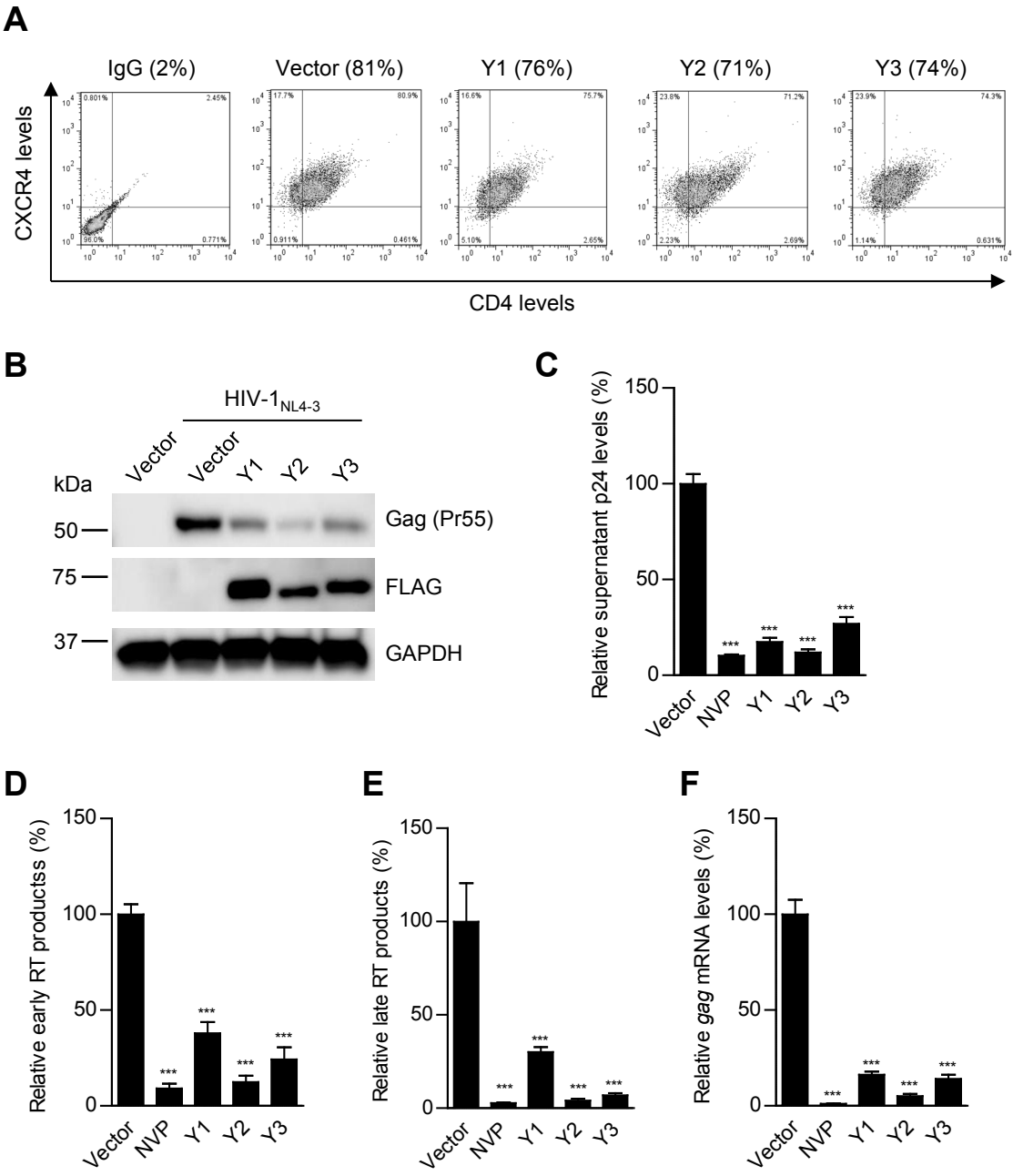
A
IgG (2%)
Vector (81%)
Y1 (76%)
Y2 (71%)
Y3 (74%)
CXCR4 levels
CD4 levels
B
HIV-1NL4-3
Vector
Vector
Y1
Y2
Y3
kDa
50
75
37
Gag (Pr55)
FLAG
GAPDH
C
Relative supernatant p24 levels (%)
150
100
50
0
***
Vector
NVP
Y1
Y2
Y3
D
Relative early RT productss (%)
E
Relative late RT products (%)
F
Relative gag mRNA levels (%)

Fig. 3

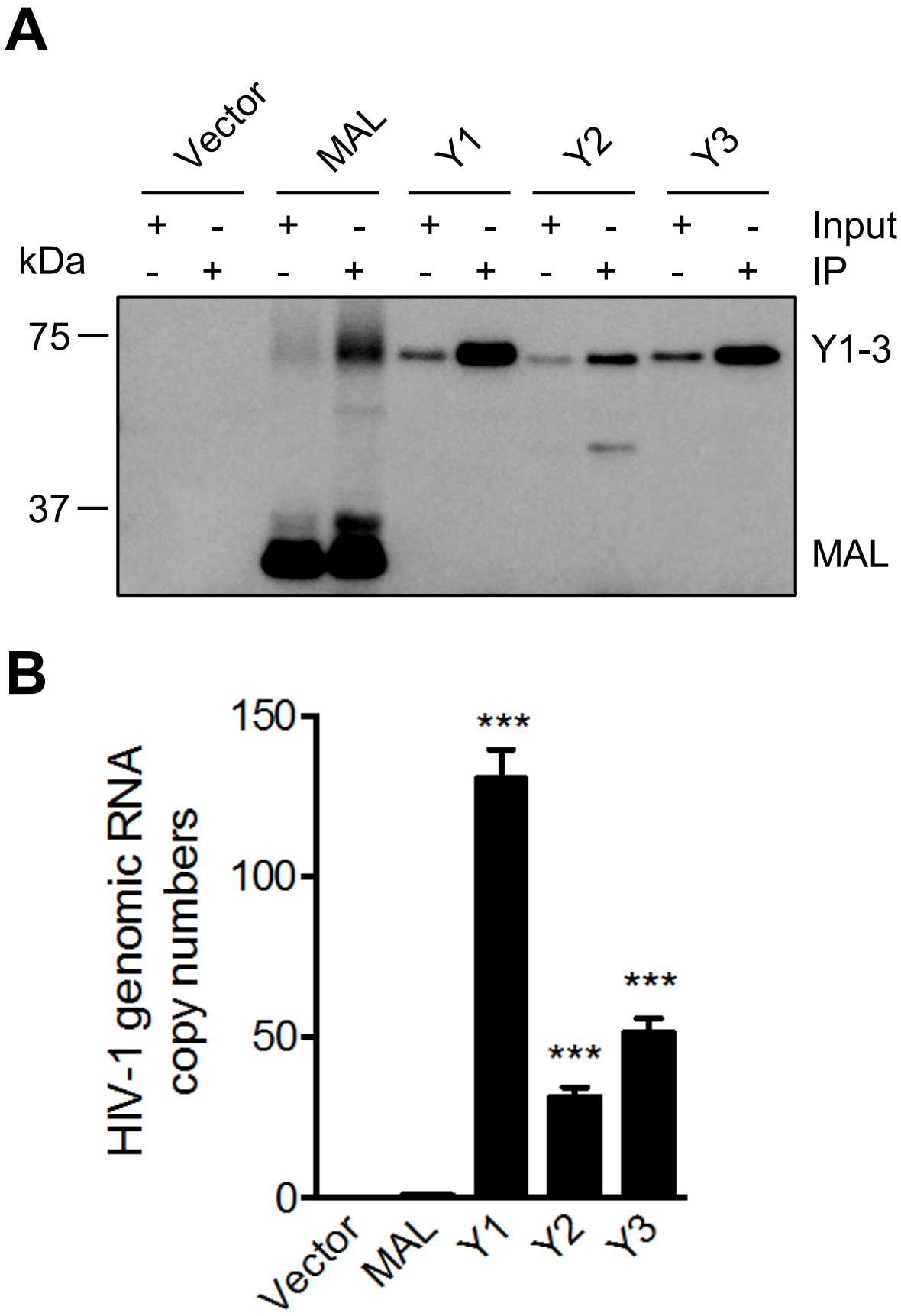
A
Vector
MAL
Y1
Y2
Y3
+ - + - + - + - + -
Input
kDa
- + - + - + - + - +
IP
75
37
Y1-3
MAL
B
HIV-1 genomic RNA copy numbers
150
100
50
0
***
***
***
Vector
MAL
Y1
Y2
Y3

Fig. 4

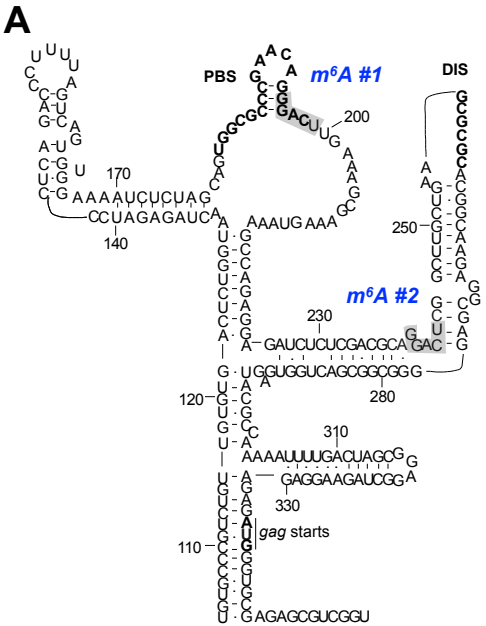

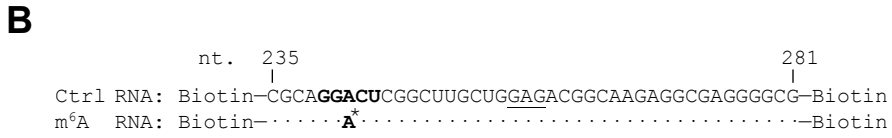

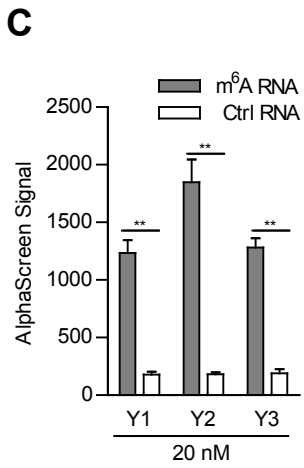

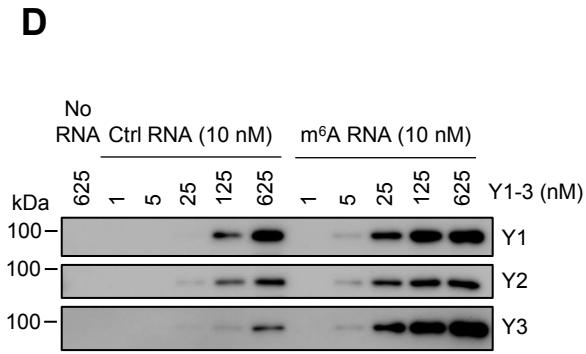

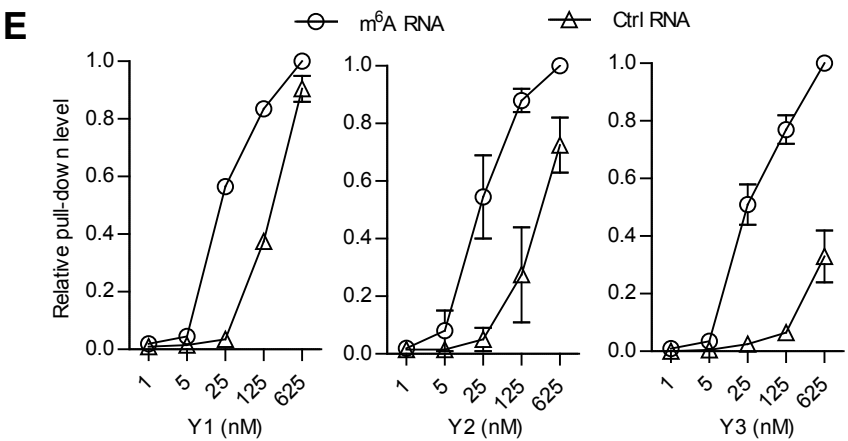

F

50% pull-down efficiency (nM)	Y1	Y2	Y3
m6A RNA	26	25	31
Ctrl RNA	178	326	>625

Fig. 5

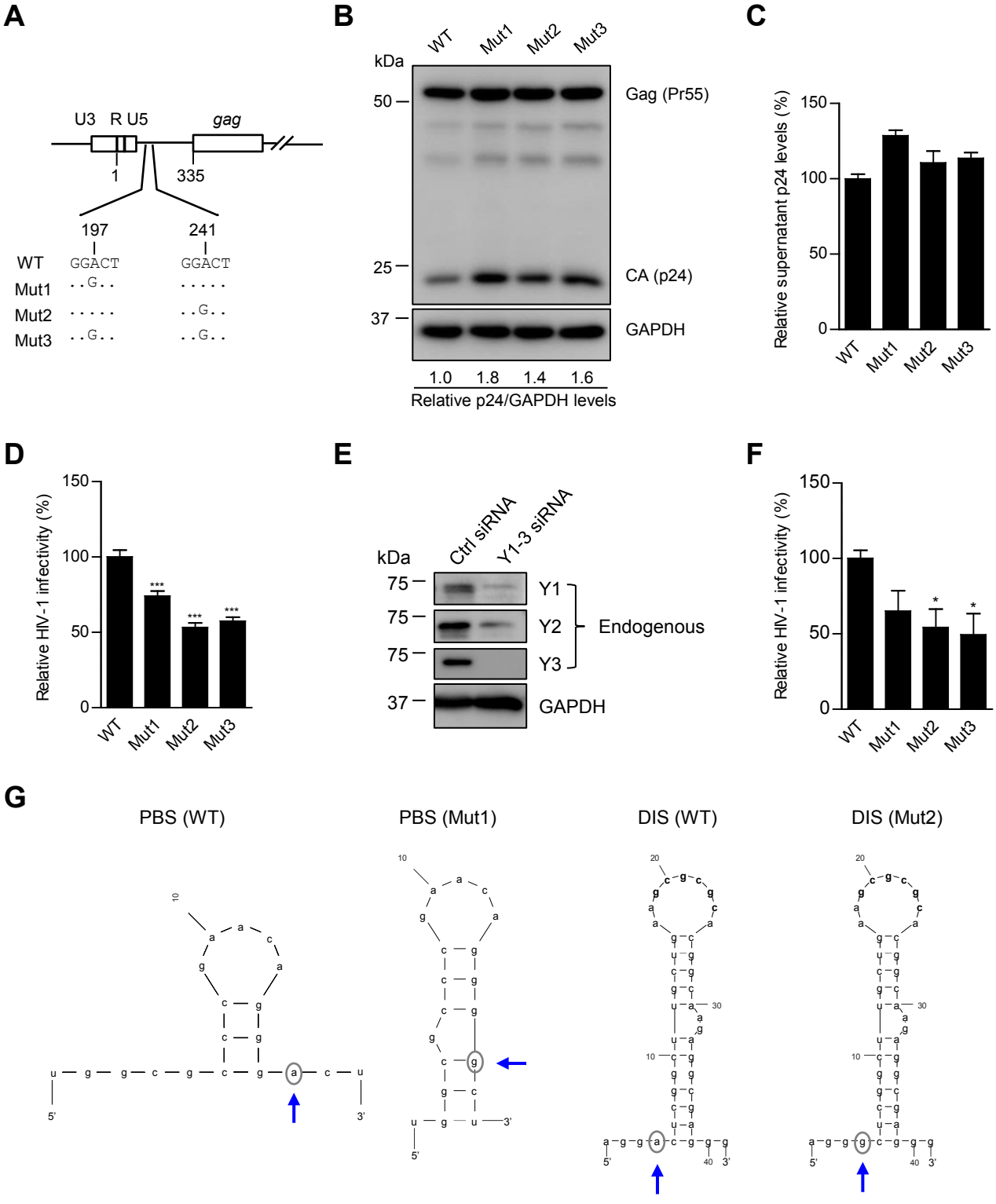
A
U3 R U5
gag
1
335
197
241
WT GGACT GGACT
Mut1 ..G.. .....
Mut2 ....G..
Mut3 ..G.. ..G..
B
WT
Mut1
Mut2
Mut3
kDa
50
25
37
Gag (Pr55)
CA (p24)
GAPDH
1.0 1.8 1.4 1.6
Relative p24/GAPDH levels
C
Relative supernatant p24 levels (%)
150
100
50
0
WT
Mut1
Mut2
Mut3
D
Relative HIV-1 infectivity (%)
150
100
50
0
***
***
***
WT
Mut1
Mut2
Mut3
E
Ctrl siRNA
Y1-3 siRNA
kDa
75
75
75
37
Y1
Y2
Y3
Endogenous
GAPDH
F
Relative HIV-1 infectivity (%)
150
100
50
0
*
*
WT
Mut1
Mut2
Mut3
G
PBS (WT)
PBS (Mut1)
DIS (WT)
DIS (Mut2)
5'
3'

Fig. 6

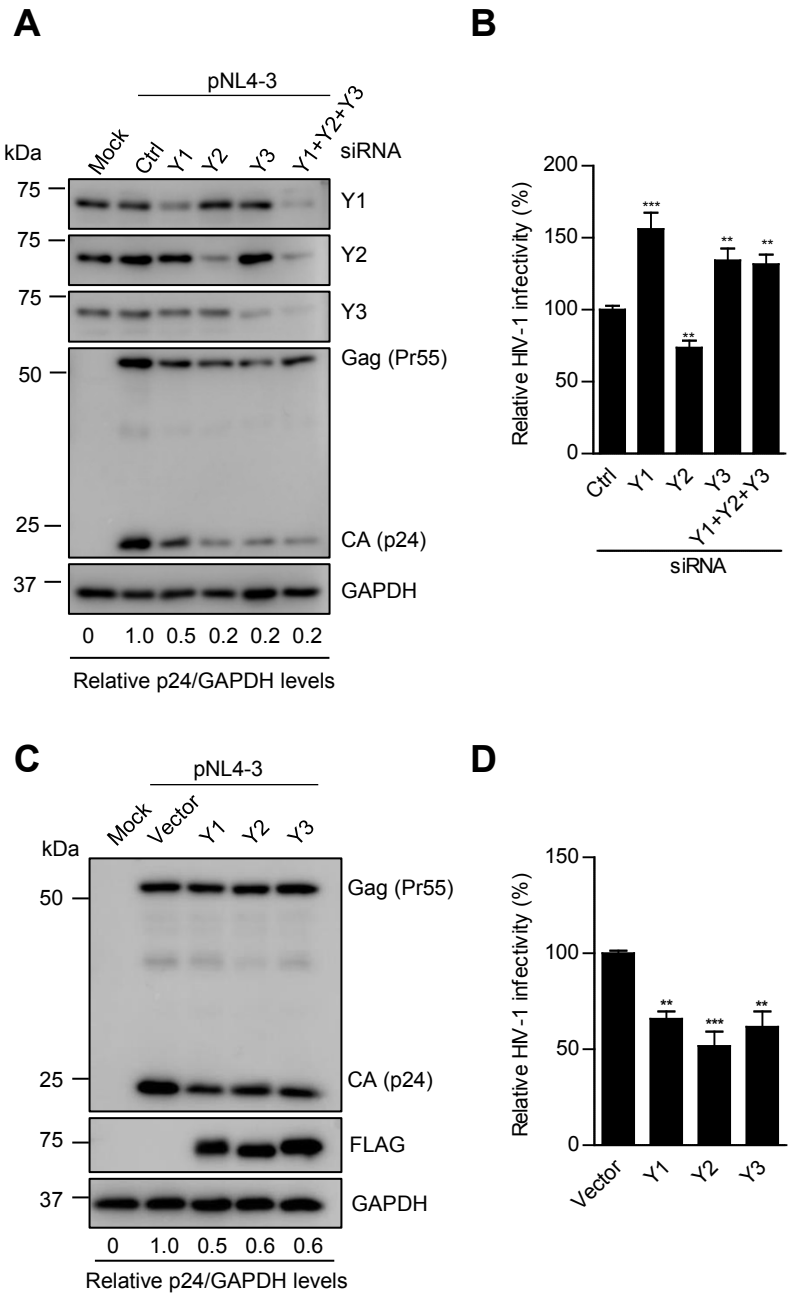
A
pNL4-3
kDa
Mock
Ctrl
Y1
Y2
Y3
Y1+Y2+Y3
siRNA
75
75
75
50
25
37
Y1
Y2
Y3
Gag (Pr55)
CA (p24)
GAPDH
0 1.0 0.5 0.2 0.2 0.2
Relative p24/GAPDH levels
B
Relative HIV-1 infectivity (%)
200
150
100
50
0
***
**
**
**
Ctrl
Y1
Y2
Y3
Y1+Y2+Y3
siRNA
C
pNL4-3
kDa
Mock
Vector
Y1
Y2
Y3
50
25
75
37
Gag (Pr55)
CA (p24)
FLAG
GAPDH
0 1.0 0.5 0.6 0.6
Relative p24/GAPDH levels
D
Relative HIV-1 infectivity (%)
150
100
50
0
**
***
**
Vector
Y1
Y2
Y3

Fig. 7

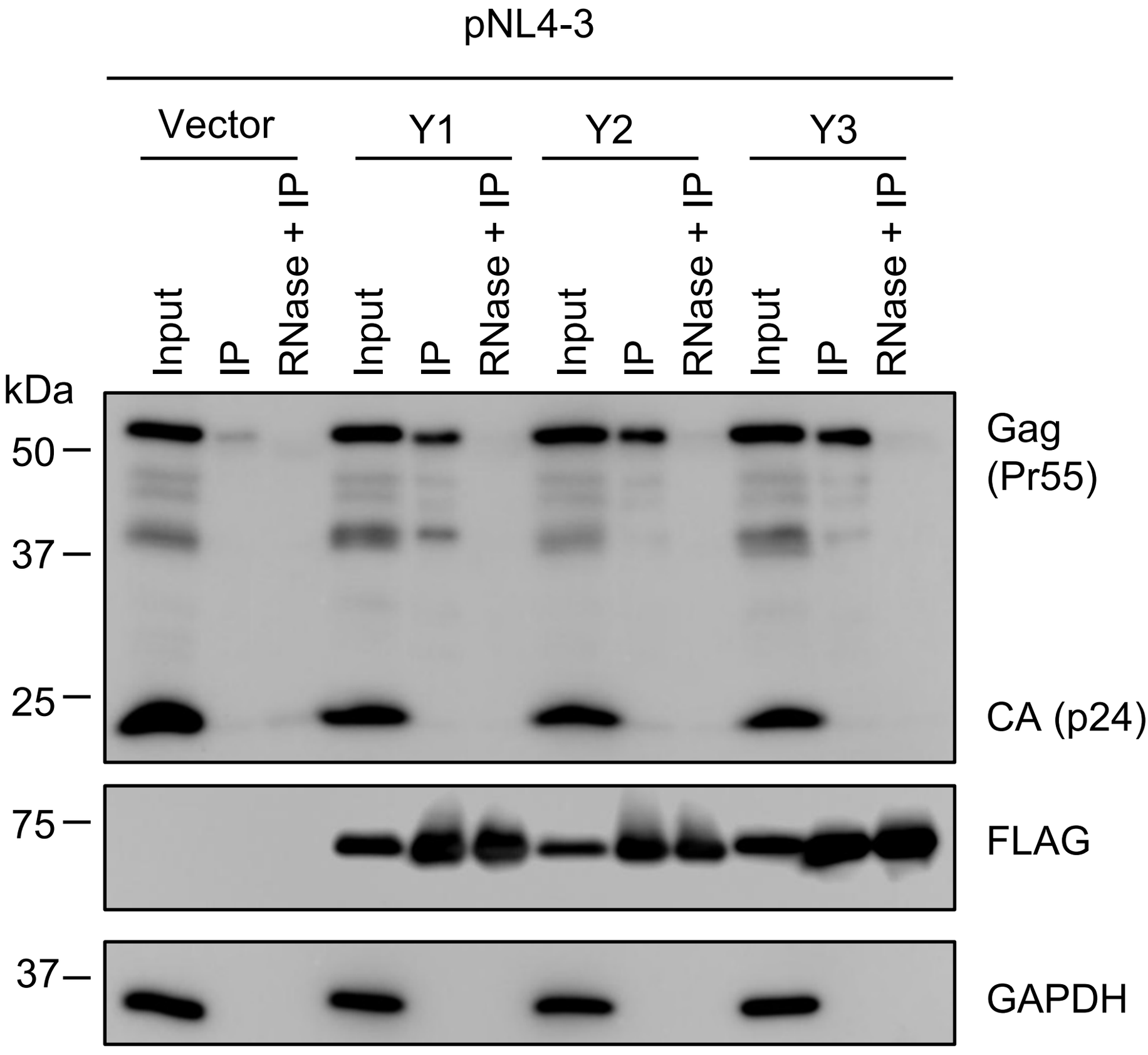
pNL4-3
Vector
Y1
Y2
Y3
Input
IP
RNase + IP
kDa
50
37
25
75
37
Gag (Pr55)
CA (p24)
FLAG
GAPDH

Fig. 8

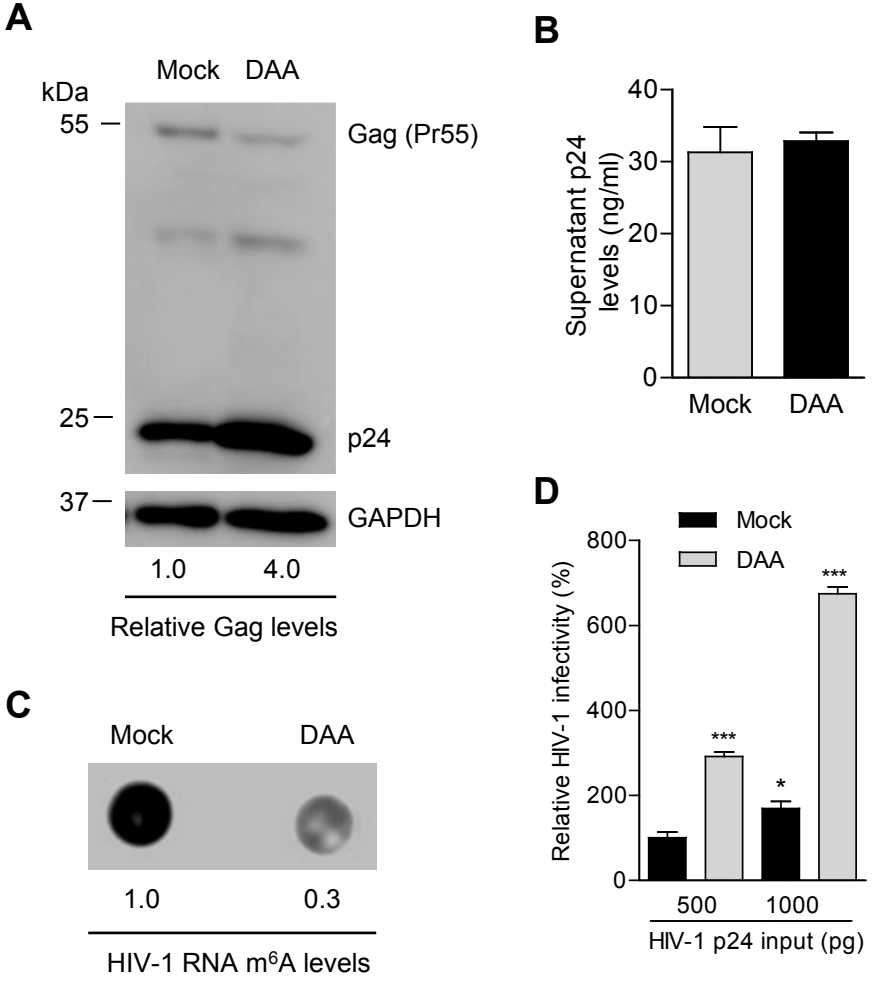
A
Mock
DAA
kDa
55
Gag (Pr55)
25
p24
37
GAPDH
1.0
4.0
Relative Gag levels
B
Supernatant p24 levels (ng/ml)
40
30
20
10
0
Mock
DAA
C
Mock
DAA
1.0
0.3
HIV-1 RNA m6A levels
D
Mock
DAA
Relative HIV-1 infectivity (%)
800
600
400
200
0
***
*
***
500
1000
HIV-1 p24 input (pg)